JOURNAL OF GUIDANCE, CONTROL, AND DYNAMICS
Vol. 21, No. 3, May–June 1998

Escape from Gyrostat Trap States

Christopher D. Hall*
U.S. Air Force Institute of Technology, Wright–Patterson Air Force Base, Ohio 45433

Some results are presented on the dynamics of gyrostats containing two axisymmetric rotors where one of the rotors is viscously damped and the other is subject to a controllable torque. The purpose of this arrangement is to investigate the use of internal torques to enable a spacecraft to escape from a trap state. Suppose the spacecraft is intended to operate in a state in which the primary rotor $\mathcal{R}_1$ has a specified angular momentum and the other rotor $\mathcal{R}_2$, subject only to internal viscous torques, is not spinning relative to the spacecraft reference frame. Normally this state is asymptotically stable because of the damping. It is possible that a different asymptotically stable state exists satisfying these conditions on the rotor momenta, in much the same way that a single-spinner may spin in either direction about its major axis. If the spacecraft becomes trapped in the alternate state, it is necessary to help it escape. In an earlier study, a pulsing procedure was proposed. Herein we show that periodic torquing of the primary rotor may lead to escape but generally is rather ineffective. An alternative escape procedure is presented that essentially is guaranteed to lead to escape. Unlike the local analysis that suggests the pulsing procedure, the procedure used here is based on a global analysis of the rotational dynamics.

Introduction

THE study of trap states of dual-spin spacecraft was introduced by Scher and Farrenkopf[1] in 1974 and has been continued by several authors.[2–11] One of the trap states discussed by Scher and Farrenkopf[1] was termed a minimum energy trap and is comparable to the major axis spin of a single quasirigid body.[12] For a single-spinner, the sense of spin about the major axis may be important, so that a spin in the wrong sense could be considered a minimum energy trap state. This situation has occurred in practice and has been investigated by Kaplan and Cenker,[13] who proposed a moving-mass configuration to control the reorientation of a quasirigid body from minor to major axis spin with desired final sense of rotation. The principal physical cause of the minimum energy trap states is the existence of energy dissipation mechanisms on spacecraft. The effects of energy dissipation on the motion of dual-spin spacecraft have been studied by many authors.[14–20] Most of the analyses are based on local analysis or on simulation results for particular dual-spin models. One especially useful class of models is the gyrostat, in which one or more rigid axisymmetric rotors is attached to a rigid platform. These models are distinguished by the fact that, in the absence of axial torques on the rotors, the equations of motion are integrable. As with the rigid body, one may consider the qualitative effects of energy dissipation on the rotational dynamics, but the details are more complicated. The text by Hughes[12] includes a detailed analysis of these effects for quasirigid gyrostats.

Scher and Farrenkopf[1] suggested the use of a periodic torquing of the rotor to escape from the minimum energy trap and illustrated the procedure using simulation. Note that their model is not a gyrostat because the platform is unbalanced and the rotor is asymmetric. However, as has been discussed in Ref. 9, trap states may occur in gyrostat models as well. We study the problem of escaping from a minimum energy state using a gyrostat model with two rotors: One is subject only to an internal viscous damping torque, and the other is subject to an internal controlled motor torque. This model is motivated by Hubert's use of a viscously damped rotor to model the energy dissipation in a dual-spin spacecraft.[5]

Presented as AAS Paper 95-337 at the AAS/AIAA Astrodynamics Conference, Halifax, NS, Canada, Aug. 14–17, 1995; received Aug. 7, 1996; revision received Jan. 12, 1998; accepted for publication Jan. 29, 1998.

*Assistant Professor of Aerospace and Systems Engineering, Graduate School of Engineering, Department of Aeronautics and Astronautics; currently Assistant Professor, Department of Aerospace and Ocean Engineering, Virginia Polytechnic Institute and State University, Blacksburg, VA 24061. Associate Fellow AIAA.

We begin with the equations of motion, which are essentially those derived in Ref. 21. A discussion of the relative equilibrium motions and their stability properties follows. We then discuss two methods of escaping from an undesirable trap state. One method uses a periodic torque similar to that described in Ref. 1, but this is relatively ineffective in the presence of significant damping. A second method is similar to the approach used by Hubert[5] but is more general and is based on the noncanonical Hamiltonian description of gyrostat dynamics developed in Ref. 21. This method is highly effective and results in a satisfactory escape regardless of the strength of the damping or the magnitude of the motor torque.

Equations of Motion

The model studied consists of a rigid platform with two axisymmetric rotors constrained to relative rotation about their axes of symmetry; however, we begin with the equations of motion for an N-rotor gyrostat (see Fig. 1). For the $N = 2$ case presented in detail, one rotor is subject to a controlled motor torque, and the second rotor is subject only to viscous damping torque. Because the control torques normally are larger than the environmental disturbance torques, we ignore all external torques. For a more detailed derivation, see Ref. 21.

All vectors and tensors are expressed in a platform-fixed, nonprincipal frame, termed the pseudoprincipal frame, which is determined as follows: The rotor axial vectors $\boldsymbol{a}_j$ are collected as the columns of a $3 \times N$ matrix $A = [\boldsymbol{a}_1 \ \cdots \ \boldsymbol{a}_N]$. The moment-of-inertia matrix of the gyrostat (including the rotors) is denoted I, and the axial moments of inertia of the rotors are collected as an $N \times N$ diagonal matrix I_s. The pseudoprincipal frame is chosen so that the matrix $J = I - AI_sA^T$ is diagonal. The components of the system angular momentum vector may be written as the column vector

$$\boldsymbol{h} = I\boldsymbol{\omega} + AI_s\boldsymbol{\omega}_s \tag{1}$$

where $\boldsymbol{\omega}_s$ is an $N \times 1$ matrix containing the angular velocities of the rotors relative to the platform. The angular momentum $\boldsymbol{h}$ satisfies the differential equation

$$\dot{\boldsymbol{h}} = -\boldsymbol{\omega}^{\times}\boldsymbol{h} \tag{2}$$

The axial rotor momenta relative to inertial space may be written as the $N \times 1$ matrix

$$\boldsymbol{h}_a = I_sA^T\boldsymbol{\omega} + I_s\boldsymbol{\omega}_s \tag{3}$$

These are subject to internal axial torques $\boldsymbol{g}_a$ applied by the platform, so that

$$\dot{\boldsymbol{h}}_a = \boldsymbol{g}_a \tag{4}$$

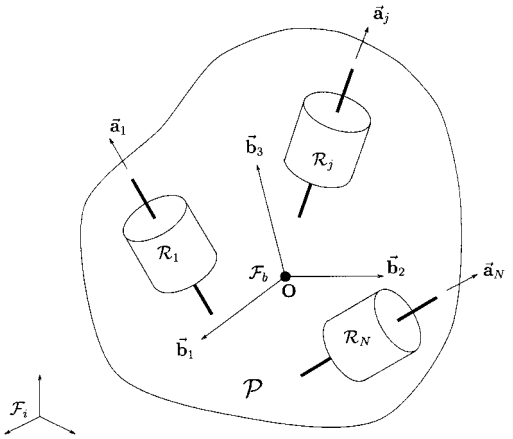

Fig. 1 *N*-rotor gyrostat model.

Instead of rewriting Eq. (2) in terms of $\dot{\boldsymbol{\omega}}$, we choose to eliminate $\boldsymbol{\omega}$ and rearrange the system of equations to obtain

$$\dot{\boldsymbol{h}} = \boldsymbol{h}^{\times} J^{-1}(\boldsymbol{h} - A\boldsymbol{h}_a) \tag{5}$$

The term $J^{-1}(\boldsymbol{h} - A\boldsymbol{h}_a)$ may be recognized as the platform angular velocity $\boldsymbol{\omega}$ and may be expressed as the gradient, with respect to $\boldsymbol{h}$, of a scalar function H_o defined as

$$H_o = \tfrac{1}{2}\boldsymbol{h}^T J^{-1}\boldsymbol{h} - \boldsymbol{h}_a^T A^T J^{-1}\boldsymbol{h} \tag{6}$$

Thus, Eq. (5) may be written as

$$\dot{\boldsymbol{h}} = \boldsymbol{h}^{\times}\nabla H_o \tag{7}$$

which is a noncanonical Hamiltonian system. Briefly, a noncanonical Hamiltonian system is a system of equations that develops from a Poisson bracket but is not directly expressed in the canonical form of

$$\dot{\boldsymbol{q}} = \frac{\partial H}{\partial \boldsymbol{p}}, \qquad \dot{\boldsymbol{p}} = -\frac{\partial H}{\partial \boldsymbol{q}}$$

As in Ref. 21, we nondimensionalize by setting $\boldsymbol{h} = h\boldsymbol{x}$, $\boldsymbol{h}_a = h\boldsymbol{\mu}$, and dividing the inertias by tr J. The torque-free kinetic equations of motion for this system may be put into a dimensionless, noncanonical Hamiltonian form as

$$\dot{\boldsymbol{x}} = \boldsymbol{x}^{\times}\nabla H \tag{8}$$

$$\dot{\boldsymbol{\mu}} = \boldsymbol{\varepsilon} \tag{9}$$

where $\boldsymbol{x}$ is the angular momentum vector, H is the Hamiltonian, $\boldsymbol{\mu}$ is the $N \times 1$ vector of rotor momenta, and $\boldsymbol{\varepsilon}$ is the $N \times 1$ vector of internal torques applied to the rotors by the platform. Conservation of angular momentum is expressed as

$$C = \boldsymbol{x}^T\boldsymbol{x}/2 = \tfrac{1}{2} \tag{10}$$

which is a special type of first integral known as a Casimir function.[22] The ∇ operator is with respect to the dimensionless angular momentum $\boldsymbol{x}$, and the Hamiltonian H is

$$H = \tfrac{1}{2}\boldsymbol{x}^T J^{-1}\boldsymbol{x} - \boldsymbol{\mu}^T A^T J^{-1}\boldsymbol{x} + f(C) \tag{11}$$

which satisfies

$$\dot{H} = \boldsymbol{\varepsilon}^T \frac{\partial H}{\partial \boldsymbol{\mu}} = -\boldsymbol{\varepsilon}^T A^T J^{-1}\boldsymbol{x} \tag{12}$$

Note that $f(C)$ in the definition of the Hamiltonian represents an arbitrary function of C that may be used to simplify the Hamiltonian. As shown in Ref. 21, addition of this term has no effect on the equations of motion. It is convenient to take $f(C) = -C/J_1$ and define two inertia parameters by

$$i_2 = \frac{J_1 - J_2}{J_1 J_2}, \qquad i_3 = \frac{J_1 - J_3}{J_1 J_3} \tag{13}$$

in which case

$$H = \tfrac{1}{2}\boldsymbol{x}^T \hat{J}\boldsymbol{x} - \boldsymbol{\mu}^T A^T J^{-1}\boldsymbol{x} \tag{14}$$

where

$$\hat{J} = \begin{bmatrix} 0 & 0 & 0 \\ 0 & i_2 & 0 \\ 0 & 0 & i_3 \end{bmatrix} \tag{15}$$

The preceding development is general and is applicable to N-rotor gyrostats. In the examples to follow, we restrict attention to a two-rotor gyrostat where $\mathcal{R}_1$ is controlled, hence ε_1 is the control variable, and $\mathcal{R}_2$ is viscously damped. In this case, the damping torque for the viscously damped rotor $\mathcal{R}_2$ is

$$\varepsilon_2 = -\gamma_2\left[\mu_2 - I_{s2}\boldsymbol{a}_2^T J^{-1}(\boldsymbol{x} - A\boldsymbol{\mu})\right] \tag{16}$$

where $\gamma_2 > 0$ is a dimensionless damping coefficient, and the term in brackets is the angular momentum of $\mathcal{R}_2$ relative to the platform. At equilibrium, $\mathcal{R}_2$ will be at rest with respect to the body frame, i.e., in the all-spun condition, with

$$\mu_{2as} = I_{s2}\boldsymbol{a}_2^T J^{-1}(\boldsymbol{x} - A\boldsymbol{\mu}) \tag{17}$$

In the limit as $I_{s2} \to 0$, the equilibrium rotor momentum also goes to zero. This is a useful analytical model for considering the effects of an energy sink on the platform of a single-rotor gyrostat.

Example. The specific dimensionless parameters of the two-rotor gyrostat used for the numerical calculations are the same as those used in Ref. 23. The principal moments of inertia are $(I_1, I_2, I_3) = (100, 70, 40)/210$. The rotor axial moments of inertia are $I_{s1} = 15/210$ and $I_{s2} = 5/210$. (The divisor 210 is the characteristic moment of inertia tr I used in the nondimensionalization[21]) The rotor axis vectors in the principal frame are $\boldsymbol{a}_1 = \sqrt{3}(1, 1, 1)/3$ and $\boldsymbol{a}_2 = (-1, -2, 2)/3$. The rotation matrix that diagonalizes $J = I - AI_sA^T$ is

$$Q = \begin{bmatrix} 0.9827 & 0.1707 & 0.0722 \\ -0.1776 & 0.9785 & 0.1045 \\ -0.0528 & -0.1156 & 0.9915 \end{bmatrix} \tag{18}$$

The diagonal elements of J in this frame are (0.4560, 0.2954, 0.1533). The rotor axis vectors in the nonprincipal frame are $\boldsymbol{a}_1 = (0.4343, 0.5968, 0.6747)$ and $\boldsymbol{a}_2 = (-0.2444, -0.7863, 0.5675)$.

Equilibrium Motions

The enumeration and characterization of the equilibrium motions of dual-spin spacecraft have been undertaken repeatedly using various techniques. Except for a few simple cases, one must eventually resort to numerical techniques to discover both the location of the equilibria and the stability properties. In the following subsection, we describe briefly a technique for carrying out the necessary computations. The technique has the advantage that it leads nicely into a stability analysis of the equilibria because some of the same calculations are involved. The section concludes with a description of the possibilities of competing trap states.

It is well known[12] that there are either two, four, or six equilibria, depending on the value of the rotor momentum $\boldsymbol{\mu}$. As in Ref. 21, we use the symbols $O_\mu^{\pm}$, $U_\mu^{\pm}$, and $P_\mu^{\pm}$ to denote oblate, unstable, and prolate equilibria, respectively. These are directly analogous to the rigid-body equilibria, and in the following section we use this fact to develop an efficient method of computing the equilibria and determining their stability.

Computation

We begin by considering equilibrium motions with $\boldsymbol{\varepsilon} = \boldsymbol{0}$, i.e., $\varepsilon_1 = 0$ and $\gamma_2 = 0$. Unlike the canonical case, the condition $\nabla H = 0$ is not necessary for an equilibrium of a noncanonical Hamiltonian system. From Eq. (8), it is evident that if $\nabla H = \lambda\nabla C$, where λ is a constant Lagrange multiplier, then $\dot{\boldsymbol{x}} = 0$, and the system is in equilibrium. Thus, equilibrium points are critical points of the augmented Hamiltonian

$$F(\boldsymbol{x}, \lambda; \boldsymbol{\mu}) = H(\boldsymbol{x}; \boldsymbol{\mu}) - \lambda C(\boldsymbol{x}) \tag{19}$$

with respect to $\boldsymbol{x}$ and the Lagrange multiplier λ. The condition for an equilibrium can be expressed as

$$\boldsymbol{F}(\boldsymbol{x}, \lambda; \boldsymbol{\mu}) = DF(\boldsymbol{x}, \lambda; \boldsymbol{\mu}) = \begin{bmatrix} (\hat{J} - \lambda 1)\boldsymbol{x} - J^{-1}A\boldsymbol{\mu} \\ 1 - \boldsymbol{x}^T\boldsymbol{x} \end{bmatrix} = 0 \quad (20)$$

where $D(\,) = \partial(\,)/\partial(\boldsymbol{x}, \lambda)$. Because we want to compute the equilibrium solutions $(\boldsymbol{x}_e, \lambda_e)$ as functions of $\boldsymbol{\mu}$, we apply a continuation procedure such as the Euler–Newton method.[24]

This procedure requires a known starting solution $\boldsymbol{x}_e = \boldsymbol{x}_o(\boldsymbol{\mu}_o)$ and associated $\lambda_e = \lambda_o$. A suitable step size in $\boldsymbol{\mu}$ is chosen, denoted $\Delta\boldsymbol{\mu}$, so that $\boldsymbol{\mu} = \boldsymbol{\mu}_o + \Delta\boldsymbol{\mu}$. Letting $\boldsymbol{z} = (\boldsymbol{x}, \lambda)$, the Euler step in this procedure is

$$\boldsymbol{z}_n = \boldsymbol{z}_o - [D\boldsymbol{F}(\boldsymbol{z}_o, \boldsymbol{\mu}_o)]^{-1}\frac{\partial \boldsymbol{F}}{\partial \boldsymbol{\mu}}(\boldsymbol{z}_o, \boldsymbol{\mu}_o)\Delta\boldsymbol{\mu} \quad (21)$$

which is refined in the Newton iteration

$$\boldsymbol{z}_{n+1} = \boldsymbol{z}_n - [D\boldsymbol{F}(\boldsymbol{z}_n, \boldsymbol{\mu})]^{-1}\boldsymbol{F}(\boldsymbol{z}_n, \boldsymbol{\mu}) \quad (22)$$

The Newton step may be too large, with the result that

$$\|\boldsymbol{F}(\boldsymbol{z}_{n+1}, \boldsymbol{\mu})\| > \|\boldsymbol{F}(\boldsymbol{z}_n, \boldsymbol{\mu})\| \quad (23)$$

In this case, successively smaller steps in the Newton direction are taken until the approximation is an improvement. The Newton iteration is repeated until

$$\|\boldsymbol{F}(\boldsymbol{z}_n, \boldsymbol{\mu})\| < r \quad (24)$$

where r is a prescribed tolerance. In some cases more subtle stopping criteria may be required, especially in a neighborhood of a bifurcation point.

The derivative matrices required may be easily shown to be

$$D\boldsymbol{F} = \begin{bmatrix} \hat{J} - \lambda\mathbf{1} & -\boldsymbol{x} \\ -\boldsymbol{x}^T & 0 \end{bmatrix} \quad (25)$$

and

$$\frac{\partial \boldsymbol{F}}{\partial \boldsymbol{\mu}} = \begin{bmatrix} -J^{-1}A \\ 0^T \end{bmatrix} \quad (26)$$

Note that $D\boldsymbol{F}$ is a symmetric 4×4 matrix depending on $\boldsymbol{x}$ and λ, whereas $\partial\boldsymbol{F}/\partial\boldsymbol{\mu}$ is a constant $4 \times N$ matrix.

As noted above, a starting point $\boldsymbol{z}_o(\boldsymbol{\mu}_o)$ is required. For gyrostat problems, a set of suitable starting points is the set of rigid-body equilibria given by $\boldsymbol{\mu}_o = 0$. As noted, for this case, the motion reduces to that of a rigid body with inertia matrix J. Thus, the equilibria for $\boldsymbol{\mu} = 0$ are simply steady spins about the pseudoprincipal axes, which are generally different from the principal axes. We denote these steady spins by $\boldsymbol{x}_e = \pm\boldsymbol{e}_i$, where $\boldsymbol{e}_i$ is the ith standard unit vector. The corresponding Lagrange multiplier λ_o is determined from the first-order conditions [Eq. (20)]. Thus, the $\boldsymbol{\mu} = 0$ starting points are as given in Table 1.

It is useful to plot the equilibrium value of the Hamiltonian as a function of the rotor momentum $\boldsymbol{\mu}$. In the single-rotor case, this results in a plane bifurcation diagram,[21] and for N-rotor gyrostats, an $N+1$ dimensional bifurcation diagram is required.[23] In the present two-rotor case, the equilibria form surfaces in $\mu_1\mu_2H$ space (see Ref. 23 for examples). However, because we are interested in the limiting case where $I_{s2} \to 0$, which implies that $\mu_2 \to 0$, we restrict the bifurcation diagrams to the $\mu_1 H$ plane. For the example gyrostat, the $\mu_1 H$ bifurcation diagram is shown in Fig. 2. In the figure, the solid curves represent stable equilibria (centers), and dashed curves denote unstable equilibria (saddles). The $O_\mu^\pm$ equilibria are asymptotically stable in the case of energy dissipation, whereas the $P_\mu^\pm$

Table 1 The $\mu = 0$ equilibrium solutions

Equilibria	z_o
$O_\mu^\pm$	$(\pm 1, 0, 0, 0)$
$U_\mu^\pm$	$(0, \pm 1, 0, j_2)$
$P_\mu^\pm$	$(0, 0, \pm 1, j_3)$

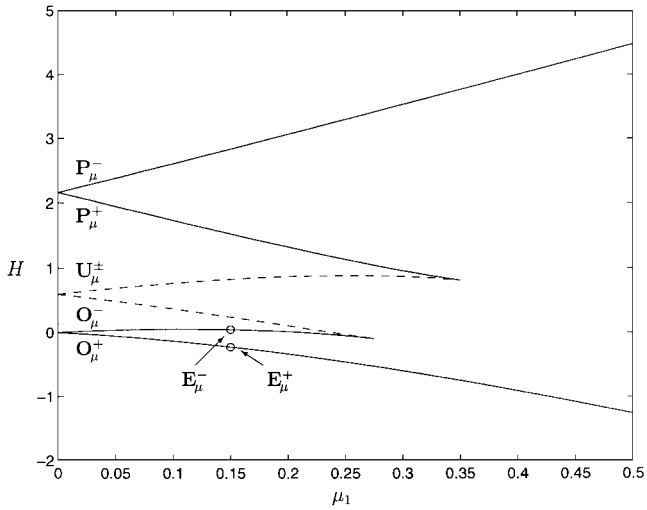

Fig. 2 The $\mu_1 H$ plane with two competing states.

equilibria are stable only in the undamped case. The $U_\mu^\pm$ equilibria are unstable in either case. The points labeled $E_\mu^\pm$ are the trap states, which are discussed in later sections. Although we only show the $\mu_1 H$ plane for $\mu_1 \geq 0$, the plane is symmetric about $\mu_1 = 0$. This fact is useful in developing strategies for escaping from trap states.

The calculation of equilibria with $\gamma_2 > 0$ requires the addition of Eq. (17), as well as adding derivatives with respect to μ_2 to the Euler–Newton algorithm. However, as noted at Eq. (17), in the limit of small I_{s2}, the solution to this equation approaches $\mu_2 = 0$.

Stability

In the absence of knowledge of other equilibria, the rigid-body equilibria provide useful starting points for the continuation procedure. A further advantage of these starting points is that the stability properties of these equilibria are known. If the inertia parameters are ordered so that $J_1 > J_2 > J_3$, then the equilibria corresponding to steady spins about the pseudoprincipal axes have the same stability properties as the associated spins for a rigid body having the J_i as principal moments of inertia. That is, $\pm\boldsymbol{e}_1$ are stable (major axis) spins, $\pm\boldsymbol{e}_2$ are unstable (intermediate axis) spins, and $\pm\boldsymbol{e}_3$ are stable (minor axis) spins. The branches emanating from these starting points retain these stability properties unless a bifurcation occurs, in which case an exchange of stability may occur. Interestingly enough, the generic bifurcations that occur in this problem are turning points in which a saddle and a center coalesce and disappear, and so, no exchange of stability occurs.

Thus, the stability of an equilibrium motion can be deduced directly, based on which rigid-body ($\boldsymbol{\mu} = 0$) branch the equilibrium is on. Alternatively, the function F defined in Eq. (19) is a candidate Lyapunov function because, in the absence of axial torques on the rotor, F is constant. Thus stability of $\boldsymbol{\varepsilon} = \mathbf{0}$ equilibria is assured if $\nabla^2 F$ is sign-definite, where the gradient is with respect to $\boldsymbol{x}$. Clearly,

$$\nabla^2 F = \hat{J} - \lambda_e 1 = \begin{bmatrix} -\lambda_e & 0 & 0 \\ 0 & i_2 - \lambda_e & 0 \\ 0 & 0 & i_3 - \lambda_e \end{bmatrix} \quad (27)$$

Therefore, because $0 < i_2 < i_3$, a sufficient condition for stability of an equilibrium is for the Lagrange multiplier to satisfy

$$\lambda_e < 0 \quad (28)$$

which is a simple test to make during the Euler–Newton continuation procedure. It turns out that only the O_μ^+ branch satisfies this condition, and $\lambda_e \geq 0$ for the other branches. In particular, we expect the O_μ^- branch to exhibit the same stability properties as the O_μ^+ branch, and so, it is unfortunate that the simple condition above does not hold. However, it is possible to prove nonlinear stability of the O_μ^- branch.

First, we note that, on this branch, λ satisfies $0 < \lambda_e < i_2 < i_3$; therefore, $\nabla^2 F$ has only one negative eigenvalue. A theorem due

Table 2 Desired state and trap state

State variable	E_μ^+	E_μ^-
μ_1	0.15	0.15
μ_2	≈ 0	≈ 0
H	−0.2259	0.0468
x_1	0.9629	−0.9435
x_2	0.2261	0.2912
x_3	0.1474	0.1580
ω_1	1.9688	−2.2120
ω_2	0.4622	0.6827
ω_3	0.3015	0.3705
ω_n	2.3667	1.9523

to Maddocks[25] states that, when the Casimir function C is parameterized by the Lagrange multiplier λ, then at a relative equilibrium, where $\partial C/\partial\lambda < 0$ and only one eigenvalue of $\nabla^2 F$ is negative, the relative equilibrium is nonlinearly stable. Substituting for $\boldsymbol{x}_e$ in terms of λ_e [using Eq. (20)] in the definition of C and taking the partial derivative with respect to λ leads to

$$\frac{\partial C}{\partial \lambda} = \boldsymbol{\mu}^T A^T J^{-1} \text{diag}\left(-\frac{1}{\lambda_e^3}, \frac{1}{(i_2-\lambda_e)^3}, \frac{1}{(i_3-\lambda_e)^3}\right) J^{-1} A \boldsymbol{\mu} \tag{29}$$

Direct calculation shows that this quantity is negative along the O_μ^- branch. This approach also applies to the P_μ^- branch, but not the P_μ^+ branch, where $\nabla^2 F$ has two negative eigenvalues.

Trap States

If two asymptotically stable equilibria exist for the same value of μ_1, we call the undesirable state a trap state. If some control procedure, such as the dual-spin turn, is used to spin up the rotor, and the final motion is in the trap state, then the spacecraft may not be able to perform its mission. For the example gyrostat, an operating condition and the alternate trap state are illustrated in Fig. 2. The two points labeled $E_\mu^\pm$ are the two asymptotically stable equilibria of interest here. The desired state E_μ^+ is on the O_μ^+ surface, and the trap state E_μ^- is on the O_μ^- surface. Linearization about equilibrium, with $\mu_2 = 0$, leads to a system with one zero and two pure imaginary eigenvalues. The natural frequencies ω_n are different for the two equilibria. The values of the dimensionless angular momenta and velocities, and the natural frequencies for the two states are given in Table 2.

Escape from a Trap State

We now consider the problem of escaping from the trap state E_μ^- with the goal of arriving at the desired state E_μ^+. As noted in the Introduction, applying a periodic torque to $\mathcal{R}_1$ may lead to a successful escape. In this section, we investigate this approach and introduce a more effective procedure. In addition, we show how to escape from E_μ^- with the goal of arriving at E_μ^+.

Periodic Torque

To see how a periodic torque may be useful, we change to local variables as follows: Let $\boldsymbol{x} = \boldsymbol{x}_e + \delta \boldsymbol{y}$ and $\boldsymbol{\mu} = \boldsymbol{\mu}_o + \epsilon \boldsymbol{\nu}$, where $\boldsymbol{\mu}_o$ is the nominal value of the rotor momentum, and $\boldsymbol{x}_e$ is one of the (possibly six) corresponding equilibrium values of the system angular momentum. The parameters δ and ϵ are introduced for bookkeeping, with δ representing the magnitude of the departure of the system angular momentum from the nominal equilibrium value and ϵ representing the magnitude of the controlled departure of the rotor momentum from the nominal value. The equations of motion for the local coordinates $\boldsymbol{y}$ are

$$\dot{\boldsymbol{y}} = \boldsymbol{x}_e^\times (\hat{J} - \lambda_e 1)\boldsymbol{y} + \epsilon (J^{-1} A \boldsymbol{\nu})^\times \boldsymbol{y} + (\epsilon/\delta)(J^{-1} A \boldsymbol{\nu})^\times \boldsymbol{x}_e + \delta \boldsymbol{y}^\times J^{-1} \boldsymbol{y} \tag{30}$$

The four terms on the right-hand side of Eq. (30) can be identified as a linear constant coefficient term, a linear time-varying term, a forcing term, and a nonlinear term. We are particularly interested in the case in which $\boldsymbol{\nu}$ is periodic, as would be the case if the driven rotor was torqued periodically. The ordering of these terms on the basis of parameters δ and ϵ is interesting. For small oscillations about the equilibrium ($\delta \ll 1$, fixed ϵ), the forcing term is largest and the nonlinear term is smallest. For large oscillations [$\delta = \mathcal{O}(1), \epsilon \ll 1$], the nonlinear term is larger than the two periodic terms. Thus, it appears that any scheme to excite the system periodically will be most effective if the periodic excitation is at the natural frequency, rather than a sub- or superharmonic. Likewise, the nonlinearity becomes important for the large oscillations, which are necessary for effecting escape. Our analysis here is limited to a numerical investigation of the effects of a periodic torque.

We consider the following approach to escape from E_μ^- and to reach E_μ^+: Excite the system by torquing $\mathcal{R}_1$ with a periodic torque at the natural frequency of E_μ^-, which is distinct from that of E_μ^+. That is, we control the motor torque as

$$\varepsilon_1 = \epsilon \sin \omega_n^- t \tag{31}$$

where ϵ is a positive constant. To determine whether the escape is effective requires examining how the state varies due to the torque. In Fig. 2, the two equilibria of interest are seen to lie in the energy wells of the saddle U_μ^+. Thus, for escape to occur, the energy level H must rise above the U_μ^+ curve and descend to E_μ^+ on the O_μ^+ curve. Therefore, it suffices to study the change of H due to the torque.

In Fig. 3, we show H vs t for two different values of damping γ_2 and with $\epsilon = 0.01$. Starting at E_μ^-, the torque is applied for 40 s (dimensionless). In both cases, escape is not achieved because H never exceeds the value at U_μ^+ for $\mu_1 = 0.15$. Note that, as $\gamma_2 \to 0$, there is negligible change in the graph of H vs t: Escape is not achievable with arbitrarily small torque.

By increasing the amplitude of the torque, it is possible to achieve escape using this approach. In Fig. 4, H vs t is shown for $\epsilon = 0.1$ and for five different values of the damping γ_2. In all cases, the torque is applied for 40 s and then switched off. Escape evidently is achieved only for the $\gamma_2 = 0.1$ case. Note, however, that for the values of $\gamma_2 < 0.1$, the trajectories do rise above the U_μ^+ level, so that it is possible that the trajectories eventually will reach E_μ^+ or E_μ^- because of the dissipative effects of the rotor. It appears that it is important to check the state continually to determine whether escape has been achieved.

Nearly Constant Torque

Another approach is to spin up $\mathcal{R}_1$ until the trajectory passes the bifurcation point where U_μ^+ coalesces with O_μ^- (at $\mu_1 \approx 0.27$) and then reverse the torque on $\mathcal{R}_1$ until the desired value of $\mu_1 = 0.15$ is reached. Then, energy dissipation will lead to asymptotic stability of the E_μ^+ equilibrium. This can be accomplished with a constant torque, with a sign change at a specified value of $\mu_1 > 0.27$, or with a continuous torque of the form

$$\varepsilon_1 = \epsilon \tanh(\Delta\mu_1/\epsilon - t) \tag{32}$$

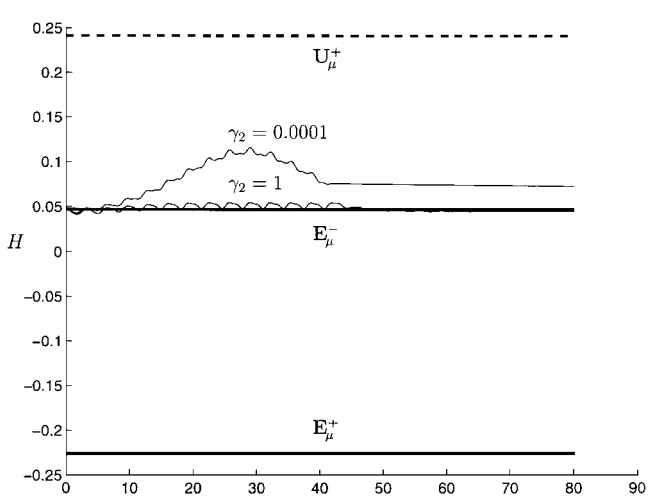

Fig. 3 H vs t with a periodic torque with amplitude $\epsilon_1 = 0.01$ and frequency $\omega_n^- = 1.9523$.

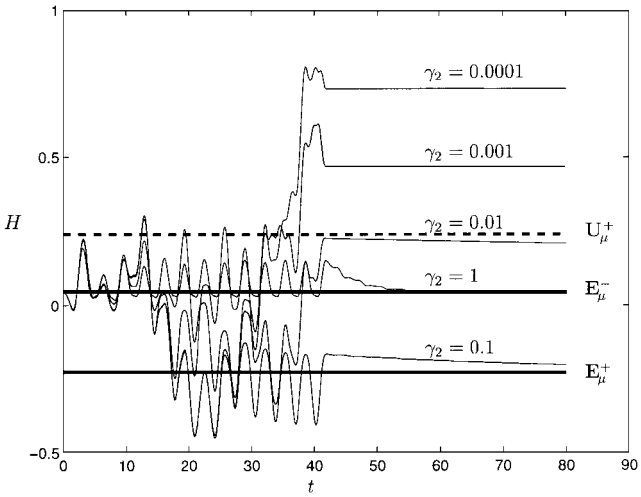

Fig. 4 H vs t with a periodic torque of amplitude $\epsilon_1 = 0.1$ and frequency $\omega_n^- = 1.9523$.

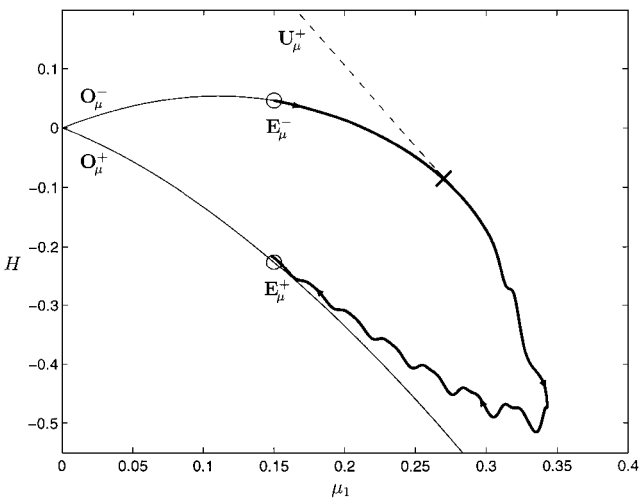

Fig. 5 The $\mu_1 H$ plane with an escape from E_μ^- to E_μ^+.

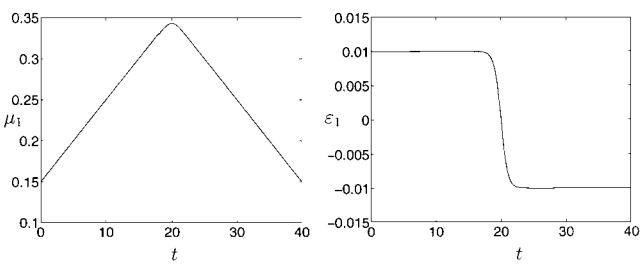

Fig. 6 Rotor momentum and motor torque vs time for constant torque escape.

where $\mu_1 = 0.15 + \Delta\mu_1$ is the desired switching point. This is similar to the approach described in Ref. 5, differing in the fact that here the trap state and desired state coexist, whereas in Ref. 5 the desired state corresponds to a high spin rate for the rotor, where only one asymptotically stable equilibrium motion exists.

Another unique aspect of the present approach is the use of the bifurcation diagram in the construction of rotational maneuvers that lead to escape. The projection of the trajectory onto the $\mu_1 H$ plane is shown in Fig. 5, and the rotor momentum and torque histories are shown in Fig. 6. Here, $\Delta\mu_1$ is taken to be 0.2, so that at the switching point the value of μ_1 is greater than the bifurcation value, which is approximately 0.27 (marked with $\times$ in Fig. 5). This approach is effective regardless of the values of γ_2 or ϵ. This approach may not be as useful in the case of systems with slightly asymmetric rotors, however, in which case it may be substantially more difficult to escape from trap states. If the inertia properties of the spacecraft are not accurately known, then a delay could be used before switching the

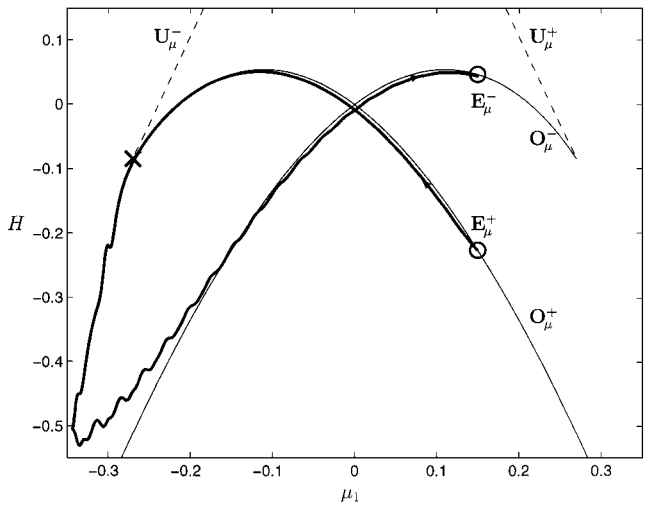

Fig. 7 The $\mu_1 H$ plane with an escape from E_μ^+ to E_μ^-.

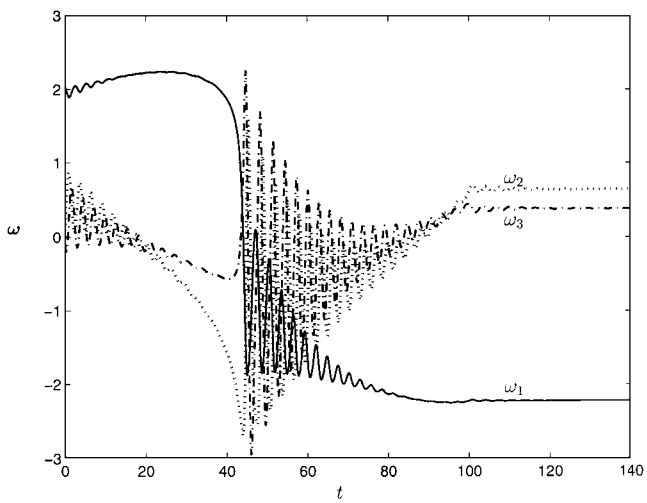

Fig. 8 Angular velocities for escape from E_μ^+ to E_μ^-.

torque direction, giving the damping mechanism more time to dissipate energy and reach the branch of asymptotically stable equilibria.

Now we consider the opposite problem of escaping from E_μ^+ with the goal of reaching E_μ^-. The approach used for escape in Fig. 5 will not work but, because the $\mu_1 H$ plane is symmetric about $\mu_1 = 0$, a similar approach will. Thus, taking

$$\varepsilon_1 = \epsilon \tanh(t - \Delta\mu_1/\epsilon) \tag{33}$$

leads to the trajectory shown in Fig. 7, where we have taken $\Delta\mu_1 = 0.5$. Here, μ_1 decreases until the switching point and then increases back to the nominal value of $\mu_1 = 0.15$. Note that, for small values of μ_1, less than about 0.15, the trajectory lies beneath the respective equilibrium branch in the $\mu_1 H$ plane. This is caused by the fact that these trajectories are actually projections onto the $\mu_1 H$ plane and follow equilibrium surfaces in the three-dimensional $\mu_1 \mu_2 H$ space. If μ_2 were identically zero, the trajectory would remain above the equilibrium branches (cf. figures in Ref. 21). The angular velocities for this escape trajectory are shown in Fig. 8. By comparing this figure with the equilibrium values of ω given in Table 2, it is evident that escape is achieved.

We conclude by noting that, as in Eq. (31) and Figs. 3 and 4, a periodic forcing also could effect an escape. However, as in the previous cases, the periodic forcing approach does not lead to certain escape, whereas the nearly constant torque of Eq. (33) does.

Conclusions

Minimum energy trap states for dual-spin spacecraft have been of interest for many years, and it has been suggested that periodically torquing the rotor at the natural frequency of the trap-state

equilibrium may be an effective escape procedure. In the presence of significant damping, this procedure may be relatively ineffective unless a large motor torque is available. Even with a large torque, it is possible that "escape" will only lead back to the original trap state. An alternative approach involving a nearly constant, arbitrarily small, torque will effect an escape for any level of damping. This approach is based on an analysis of the global dynamics and makes use of a bifurcation diagram that is based on a Hamiltonian description of the dynamics.

Acknowledgment

This work was supported by the U.S. Air Force Office of Scientific Research.

References

[1]Scher, M. P., and Farrenkopf, R. L., "Dynamic Trap States of Dual-Spin Spacecraft," *AIAA Journal*, Vol. 12, No. 12, 1974, pp. 1721–1724.

[2]Cochran, J. E., "Nonlinear Resonances in the Attitude Motion of Dual-Spin Spacecraft," *Journal of Spacecraft and Rockets*, Vol. 14, No. 9, 1977, pp. 562–572.

[3]Cochran, J. E., and Beaty, J. R., "Near-Resonant and Transition Motion of a Class of Dual-Spin Spacecraft," *Journal of the Astronautical Sciences*, Vol. 26, No. 1, 1978, pp. 19–45.

[4]Adams, G. J., "Dual-Spin Spacecraft Dynamics During Platform Spinup," *Journal of Guidance and Control*, Vol. 3, No. 1, 1980, pp. 29–36.

[5]Hubert, C. H., "Spacecraft Attitude Acquisition from an Arbitrary Spinning or Tumbled State," *Journal of Guidance and Control*, Vol. 4, No. 2, 1981, pp. 164–170.

[6]Hollars, M. G., "Minimum Energy Trap States of Dual-Spin Spacecraft," *Journal of Guidance, Control, and Dynamics*, Vol. 5, No. 3, 1982, pp. 286–290.

[7]Or, A. C., "Resonances in the Despin Dynamics of Dual-Spin Spacecraft," *Journal of Guidance, Control, and Dynamics*, Vol. 14, No. 2, 1991, pp. 321–329.

[8]Rand, R. H., Kinsey, R. J., and Mingori, D. L., "Dynamics of Spinup Through Resonance," *International Journal of Nonlinear Mechanics*, Vol. 27, No. 3, 1992, pp. 489–502.

[9]Hall, C. D., "Resonance Capture in Axial Gyrostats," *Journal of the Astronautical Sciences*, Vol. 43, No. 2, 1995, pp. 127–138.

[10]Tsui, R., and Hall, C. D., "Resonance Capture in Unbalanced Dual-Spin Spacecraft," *Journal of Guidance, Control, and Dynamics*, Vol. 18, No. 6, 1995, pp. 1329–1335.

[11]Kinsey, R. J., Mingori, D. L., and Rand, R. H., "Nonlinear Control of Dual-Spin Spacecraft During Despin Through Precession Phase Lock," *Journal of Guidance, Control, and Dynamics*, Vol. 19, No. 1, 1996, pp. 60–67.

[12]Hughes, P. C., *Spacecraft Attitude Dynamics*, Wiley, New York, 1986, Chap. 7.

[13]Kaplan, M. H., and Cenker, R. J., "Control of Spin Ambiguity During Reorientation of an Energy Dissipating Body," *Journal of Spacecraft and Rockets*, Vol. 10, No. 12, 1973, pp. 757–760.

[14]Mingori, D. L., "Effects of Energy Dissipation on the Attitude Stability of Dual-Spin Satellites," *AIAA Journal*, Vol. 7, No. 1, 1969, pp. 20–27.

[15]Bainum, P. M., Fuechsel, P. G., and Mackison, D. L., "Motion and Stability of a Dual-Spin Satellite with Nutation Damping," *Journal of Spacecraft and Rockets*, Vol. 7, No. 6, 1970, pp. 690–696.

[16]Spencer, T. M., "Energy-Sink Analysis for Asymmetric Dual-Spin Spacecraft," *Journal of Spacecraft and Rockets*, Vol. 11, No. 7, 1974, pp. 463–468.

[17]Kane, T. R., and Levinson, D. A., "Energy-Sink Analysis of Systems Containing Driven Rotors," *Journal of Guidance and Control*, Vol. 3, No. 2, 1980, pp. 234–238.

[18]Hubert, C. H., "Dynamics of the Generalized Dual-Spin Turn," *RCA Review*, Vol. 41, No. 3, 1980, pp. 449–471.

[19]Cochran, J. E., and Shu, P. H., "Effects of Energy Addition and Dissipation on Dual-Spin Spacecraft Attitude Motion," *Journal of Guidance, Control, and Dynamics*, Vol. 6, No. 5, 1983, pp. 368–373.

[20]Ross, I. M., "Nutational Stability and Core Energy of a Quasirigid Gyrostat," *Journal of Guidance, Control, and Dynamics*, Vol. 16, No. 4, 1993, pp. 641–647.

[21]Hall, C. D., "Spinup Dynamics of Gyrostats," *Journal of Guidance, Control, and Dynamics*, Vol. 18, No. 5, 1995, pp. 1177–1183.

[22]Olver, P. J., *Applications of Lie Groups to Differential Equations*, Springer–Verlag, New York, 1986, Chap. 6.

[23]Hall, C. D., "Momentum Transfer in Two-Rotor Gyrostats," *Journal of Guidance, Control, and Dynamics*, Vol. 19, No. 5, 1996, pp. 1157–1161.

[24]Seydel, R., *From Equilibrium to Chaos: Practical Bifurcation and Stability Analysis*, Elsevier, New York, 1988, Chap. 4.

[25]Maddocks, J. H., "On the Stability of Relative Equilibria," *Journal of Applied Mathematics*, Vol. 46, Nos. 1, 2, 1990, pp. 71–99.